RSC Advances

PAPER

View Article Online
View Journal | View Issue

Cite this: *RSC Adv.*, 2020, **10**, 44841

Assembly and functionalization of supramolecular polymers from DNA-conjugated squaraine oligomers†

Larysa Markova, Markus Probst and Robert Häner *

Received 30th November 2020
Accepted 1st December 2020

DOI: 10.1039/d0ra10117f

rsc.li/rsc-advances

DNA conjugated oligomers of organic molecules are candidates for applications in the materials and medical sciences, in diagnostics, in optical devices, for delivery or for the design of complex molecular architectures. Herein, we describe the synthesis and properties of DNA-conjugated squaraine (Sq) oligomers. The oligomers self-assemble into supramolecular polymers that are amenable to further functionalization *via* DNA hybridization, as shown by the attachment of gold nanoparticles (AuNPs).

While synthetic supramolecular polymers (SPs) were primarily designed to assemble in organic solvents, similar behaviour was later also demonstrated in an aqueous environment.[1,2] The change of solvent polarity offers possibilities to design and develop additional types of supramolecular systems and materials with diverse properties.[3,4] The tuning of such properties, however, remains challenging due to difficulties in the predictability of the self-assembly behaviour of new types of building blocks. These non-covalent interactions, however, are responsible for the dynamic nature of the supramolecular assemblies and, thus, for their structural homogeneity and integrity.[5,6] Growing structural and functional complexity is of particular importance once applications beyond a simple assembly–disassembly process are becoming a focus of interest.[7] This affects areas like the development of responsive materials,[8] drug delivery,[9] molecular sensors[10] and signalling cascades.[11] Ultimately, the design of building blocks should aim at predictability of the supramolecular interactions[12] and, at the same time, enable further functionalization of the formed SPs. One very robust way of addressing these prerequisites relies on the use of DNA as the addressable molecular building block.[13,14] Materials based on DNA base-pairing and strand hybridization show great promise for the assembly of defined nanostructures and elaborated molecular systems.[15–17] Increasing efforts are put into the synthesis and construction of hybrid materials, *e.g.* DNA-functionalized polymers that exhibit diverse properties in hydrogels,[18] responsive drug delivery systems[19] or optoelectronic devices.[20]

Recently, we reported on DNA-grafted supramolecular polymers[21] by combining oligoarenotides[22] and oligonucleotides. These hybrid building blocks allow the formation of supramolecular ribbons,[21,23] nanosheets[24] and vesicular constructs.[25,26] Typically, these systems show a high level of reversibility by either thermal denaturation or strand displacement reactions and they respond to external factors (*e.g.* temperature changes). In addition, the aforementioned supramolecular polymers are amenable to further modification, *e.g.* for the assembly of light-harvesting photonic wires.[27] Both, the ability to control the precise arrangement of functional building blocks and the process of supramolecular assembly of the oligomers, demonstrate the potential of DNA-functionalized materials, as neither pure synthetic supramolecular polymers nor DNA-only based systems can easily attain similar properties.[28,29]

Long-wavelength, water-compatible supramolecular assemblies are especially attractive for possible applications in the medical sciences and as optoelectronic devices.[30–32] Squaraine-based systems therefore represent ideal candidates for the creation of such "long-wavelength" supramolecular materials.[33–35] Squaraine dyes exhibit molar absorptivities of up to 260 000 M^{-1} cm^{-1},[36] they absorb and emit light in the long-wavelength region of the visible spectrum and possess the well-documented property of forming aggregates in aqueous solutions.[37,38] Squaraine assemblies designed for biomedical applications are primarily based on copolymer systems. For example, hydrophobic phospholipid bilayers of liposomes (nanovesicles) with embedded squaraine dyes are promising structures for near-infrared fluorescence and photoacoustic tomography imaging.[39] Here, we report the preparation of squaraine–DNA block co-oligomers, their assembly into SPs and their further derivatization with AuNPs.

Table 1 gives an overview on the squaraine–DNA block co-oligomers prepared *via* solid-phase synthesis (see ESI†).[36,40] The conjugates contain a varying number of squaraine units. As described below, this number determines whether defined SPs are formed. Formation of the SPs was followed by atomic force

Department of Chemistry and Biochemistry, University of Bern, Freiestrasse 3, 3012 Bern, Switzerland. E-mail: robert.haener@dcb.unibe.ch

† Electronic supplementary information (ESI) available: Experimental details and supporting figures and tables. See DOI: 10.1039/d0ra10117f

Table 1 Sequences of squaraine–DNA oligomers and AuNP-modified DNA strands. The molecular structure of the squaraine derivative (Sq) is shown in Scheme 1

Oligomer	Sequence
Sq1	3′-GAA GGC ACT C-Sq
Sq3	3′-GAA GGC ACT C-Sq Sq Sq
Sq6	3′-GAA GGC ACT C-Sq Sq Sq Sq Sq Sq
ON1-AuNP	3′-GAG TGC CTT CTT TTT TTT TT-AuNP
ON2-AuNP	3′-CCT GAA GTT ATT TTT TTT TT-AuNP

microscopy (AFM) and/or transmission electron microscopy (TEM). After supramolecular polymerization, complementary DNA strands modified with gold nanoparticles (AuNPs) were hybridized onto the DNA-modified SPs, as illustrated in Scheme 1. Since AuNPs are easily monitored by TEM imaging, they provide a straightforward tool to visualize the specific functionalization of the SPs *via* hybridization.[41]

In a first step, the influence of the number of squaraines present in the DNA-conjugated oligomers on the process of self-assembly into supramolecular polymers was investigated. UV/vis spectroscopy measurements indicated no well-defined type of aggregates under various conditions for oligomer **Sq1** containing only one squaraine unit (see ESI†). The band pattern of a spectrum recorded in ethanol, under which conditions a non-folded state of **Sq1** can be assumed, reveals an almost perfect overlay with the one recorded in aqueous conditions (Fig. S4A, ESI†). In addition, temperature-dependent absorption experiments (Fig. S4B†) show no significant changes in the absorbance of the sample during the heating–cooling cycles. In contrast, for oligomer **Sq3** containing 3 squaraine units an additional blue-shifted peak around 589 nm in the UV/vis absorption spectrum (Fig. S5A†) was observed. This agrees with data indicating the formation of H-aggregates, in which the transition dipole moments of the squaraine chromophores are arranged in a face-to-face fashion.[42,43] Aggregates of **Sq3** appear in AFM measurements as irregular objects (Fig. S5C†). In addition, thermal assembly/disassembly experiments (Fig. S5B†) reveal no signs of a supramolecular polymerization process of **Sq3**. Oligomer **Sq6** containing six squaraines, on the other hand, was found to form nanostructures with a well-defined, leaflet shaped morphology. Intramolecular folding and aggregation is accompanied by the splitting of the long-wavelength band in the UV/vis absorption spectrum. Based on literature data,[42,43] such behaviour agrees with an oblique orientation of transition dipole moments of the squaraine molecules. The formation of supramolecular polymers by **Sq6** was further tested by varying different parameters. Squaraines start to aggregate at a 125 mM concentration of NaCl. A further increase of the concentration to 300 mM resulted in a more pronounced splitting of the absorption bands. Even higher concentrations of salt (>400 mM NaCl) prompted the precipitation of aggregates (ESI, Fig. S6†). In samples with a concentration of NaCl ≥ 200 mM, **Sq6** exhibits a curve in the thermal assembly/disassembly experiments (see Fig. 1A). This is in agreement with a supramolecular polymerization process[44] although further work is required to identify the exact mechanism of polymerization/aggregation underlying the formation of the well-defined objects of **Sq6**. The heating/cooling cycles reveal a large hysteresis of around 20 °C (Fig. 1A), which is often observed for cooperative self-assembly processes with large kinetic barriers in the assembly or disassembly pathway.[44] The assembly/disassembly process is reversible as shown in repeated cooling/heating cycles (ESI, Fig. S7†). The before mentioned splitting of the long-wavelength absorption band occurs in the range from 35 °C to 45 °C and is best seen by comparing UV/vis spectra taken at different temperatures (Fig. 1B). The spectra also reveal that the formation of the SPs is a multi-step process. Isosbestic points are observable between 70 and 50 °C, which can be assigned to an intramolecular folding process. The supramolecular polymerization, which subsequently takes place below 50 °C, leads to more substantial changes in the spectrum leading to the above-mentioned

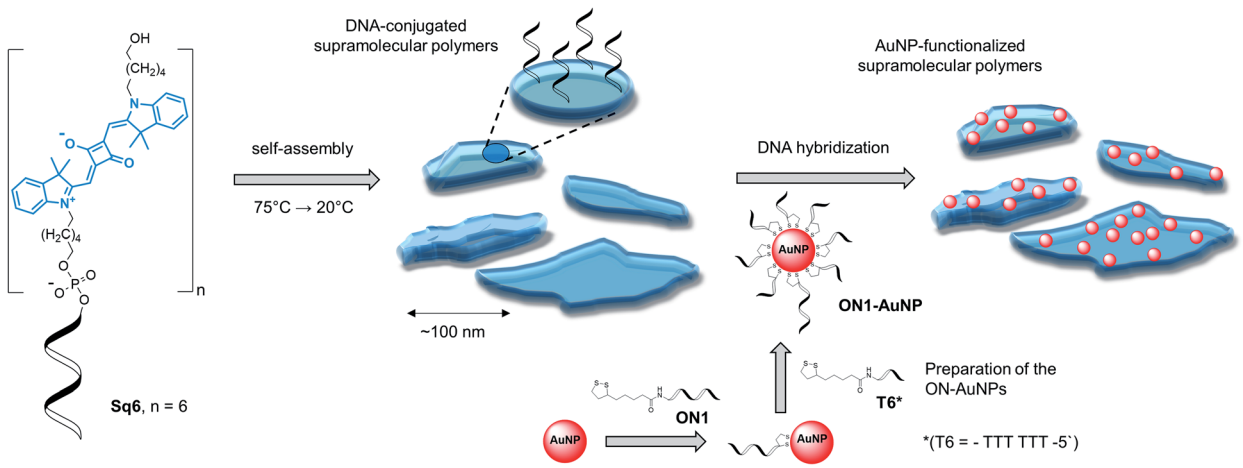

Scheme 1 Illustration of AuNP-functionalized SP formation: DNA-conjugated squaraine oligomer **Sq6** self-assembles into supramolecular polymers; subsequent hybridization of complementary AuNP-modified DNA strands leads to attachment of AuNPs to the SPs (for simplicity, DNA strands are only shown on one side of the SPs).

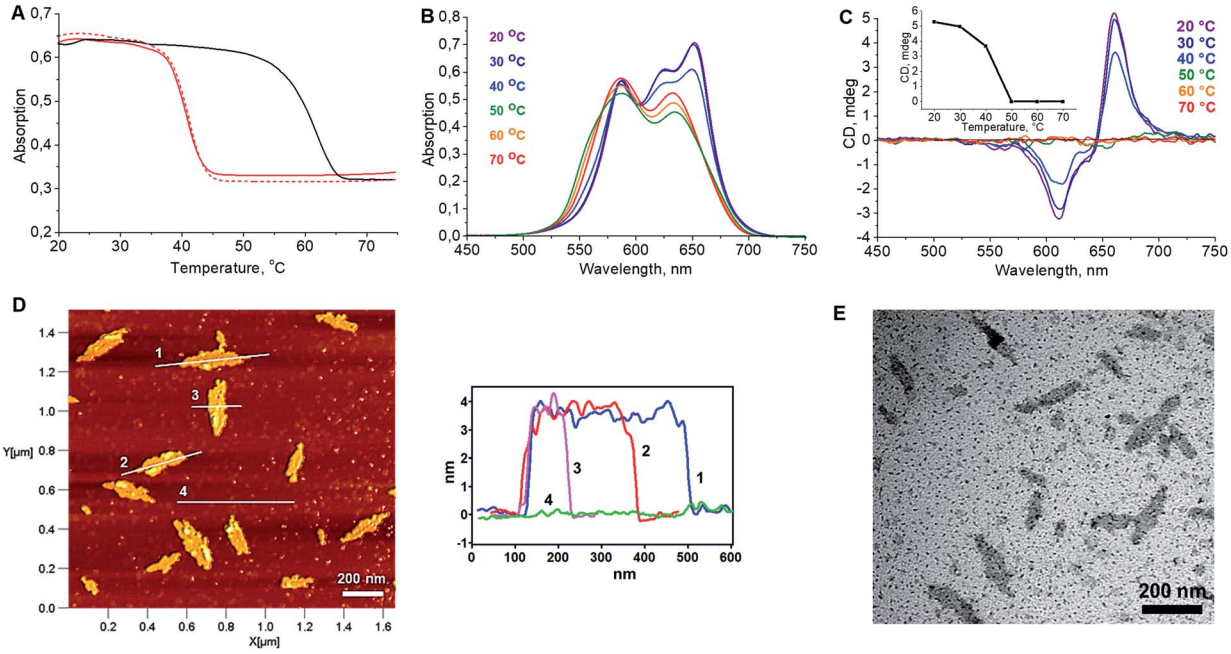

Fig. 1 (A) Cooling and heating curves recorded at $\lambda_{abs} = 660$ nm showing the reversibility of the self-assembly process; solid red: 1st cooling ramp; solid black: heating ramp; dashed red: 2nd cooling ramp; 0.5 °C min^{-1}. (B) Temperature-dependent UV/vis absorption spectra. (C) Temperature-dependent CD spectra revealing the formation of chiroptically active supramolecular polymers (inset: mdeg@660nm *vs.* Temp.). Conditions: 1 µM **Sq6**; 15% EtOH; 300 mM NaCl; 10 mM phosphate buffer, pH = 7.0. (D) AFM image of the SPs formed by oligomer **Sq6** (deposited on APTES modified mica, see ESI†) and height profiles. (E) TEM image of the **Sq6** sample (carbon-coated copper grid).

oblique orientation of transition dipole moments of the squaraine molecules.

Simultaneously, the appearance of a very distinct signal originating from exciton-coupling in the long-wavelength region of the CD spectrum is detected (Fig. 1C). AFM measurements clearly reveal the presence of well-defined objects (Fig. 1D). The dimensions of the leaflet-like structures exhibit a uniform height of about 4 nm, a typical width between 45 and 75 nm, and a typical length in the range of 100–200 nm (ESI, Fig. S10†). Objects of the same shape were also observed in TEM images (Fig. 1E) and SEM experiments confirmed the morphology (ESI, Fig. S8 and S9†).

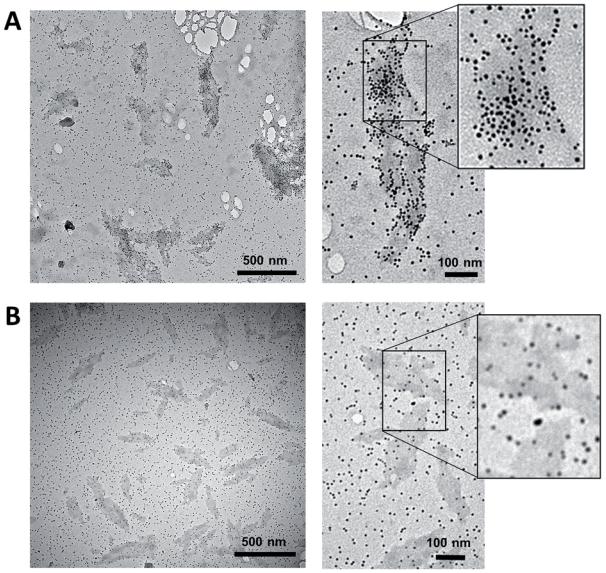

Fig. 2 (A) TEM images of the SPs functionalized by AuNPs. After the assembly of the SPs, **ON1-AuNP** (0.03 µM; conditions as in Fig. 1) was added and the mixture was left with agitation for 16 h. (B) Control experiments performed with a non-complementary, AuNP-modified oligonucleotide (**ON2-AuNP**).

The supramolecular polymers formed by the DNA-conjugated squaraine oligomer **Sq6** were functionalized by hybridization with gold nanoparticle-modified oligonucleotides. As described above, the formation of well-defined SPs is only observed when the squaraine-block reaches a length of six units. It can therefore be reasonably assumed, that the squaraine–squaraine interactions are the predominant force for the formation of the supramolecular polymers. Hence, the DNA strands in **Sq6** are expected to be accessible for hybridization with complementary DNA strands. This was verified by adding the AuNP-modified DNA oligomer **ON1-AuNP** (Table 1) to the preformed supramolecular polymers of **Sq6**. TEM images (see Fig. 2A) show the attachment and accumulation of AuNPs to the SPs. An approximation of the surface coverage (AuNP's per SP area, see ESI†) indicates values ranging from 4% to 14%. Control experiments with a non-complementary, AuNP-modified oligonucleotide (**ON2-AuNP**) showed only a small number of randomly deposited AuNPs on the SPs (Fig. 2B). This unspecific attachment of AuNPs to the surface of the TEM grid occurred in all samples, regardless of the presence or absence of Sq–DNA SPs. Obviously, subsequent washing of the grid after deposition of the samples did not remove all non-hybridized

AuNP-modified strands. Control experiments showed that this is due to the conditions required for preparing the sample (ethanol, salt and buffer, see ESI, Fig. S19†).

In conclusion, the preparation of AuNP-functionalized supramolecular polymers from DNA-conjugated squaraine oligomers has been demonstrated. Oligomers with up to six squaraine building blocks were prepared *via* solid-phase phosphoramidite chemistry. Depending on the conditions and the number of squaraine units, the oligomers self-assemble into supramolecular polymers in an aqueous medium. The formation of SPs resulted in the splitting of the long-wavelength absorption band of squaraine and was accompanied by a distinct exciton couplet centred at 660 nm in the CD spectrum. The supramolecular polymers were further modified with gold nanoparticles. The DNA-attached AuNPs hybridize sequence specifically to the DNA-modified SPs, as shown by electron microscopy. Besides allowing the sequence specific deposition of AuNPs onto the SPs, the presence of DNA also ensures water solubility of the oligomers, which may be a practical advantage for possible diagnostic or medical applications under biocompatible conditions. Furthermore, it also maintains options for applications as DNA or RNA addressed targeting and delivery devices of the described SPs.

Conflicts of interest

There are no conflicts to declare.

Acknowledgements

Financial support by the Swiss National Foundation (grant 200020_188468) is gratefully acknowledged. TEM and SEM was performed on equipment provided by Microscopy Imaging Center (MIC), University of Bern, Switzerland.

Notes and references

1 E. Krieg, M. M. C. Bastings, P. Besenius and B. Rybtchinski, *Chem. Rev.*, 2016, **116**, 2414–2477.
2 A. L. Nussbaumer, D. Studer, V. L. Malinovskii and R. Häner, *Angew. Chem., Int. Ed.*, 2011, **50**, 5490–5494.
3 N. Appukutti and C. J. Serpell, *Polym. Chem.*, 2018, **9**, 2210–2226.
4 M. Vybornyi, Y. Vyborna and R. Häner, *Chem. Soc. Rev.*, 2019, **48**, 4347–4360.
5 S. P. W. Wijnands, E. W. Meijer and M. Merkx, *Bioconjugate Chem.*, 2019, **30**, 1905–1914.
6 M. Burnworth, L. Tang, J. R. Kumpfer, A. J. Duncan, F. L. Beyer, G. L. Fiore, S. J. Rowan and C. Weder, *Nature*, 2011, **472**, 334–337.
7 N. Appukutti, J. R. Jones and C. J. Serpell, *Chem. Commun.*, 2020, **56**, 5307–5310.
8 A. W. Bosman, R. P. Sijbesma and E. W. Meijer, *Mater. Today*, 2004, **7**, 34–39.
9 H. J. Yoon and W. D. Jang, *J. Mater. Chem.*, 2010, **20**, 211–222.
10 T. L. Mako, J. M. Racicot and M. Levine, *Chem. Rev.*, 2019, **119**, 322–477.
11 M. Wehner and F. Würthner, *Nat. Rev. Chem.*, 2020, **4**, 38–53.
12 B. Baptiste, F. Godde and I. Huc, *ChemBioChem*, 2009, **10**, 1765–1767.
13 T. G. W. Edwardson, K. M. M. Carneiro, C. J. Serpell and H. F. Sleiman, *Angew. Chem., Int. Ed.*, 2014, **53**, 4567–4571.
14 H. Asanuma, H. Kashida and K. Yukiko, *Chem. Rec.*, 2014, **14**, 1055–1069.
15 M. Á. Alemán García, E. Magdalena Estirado, L.-G. Milroy and L. Brunsveld, *Angew. Chem., Int. Ed.*, 2018, **130**, 5070–5074.
16 S. K. Albert, I. Sivakumar, M. Golla, H. V. P. Thelu, N. Krishnan, Joseph Libin K. L., Ashish and R. Varghese, *J. Am. Chem. Soc.*, 2017, **139**, 17799–17802.
17 W. E. M. Noteborn, V. Saez Talens and R. E. Kieltyka, *ChemBioChem*, 2017, **18**, 1995–1999.
18 M.-A. Shahbazi, T. Bauleth-Ramos and H. A. Santos, *Adv. Ther.*, 2018, **1**, 1800042.
19 K. Liu, L. Zheng, C. Ma, R. Göstl and A. Herrmann, *Chem. Soc. Rev.*, 2017, **46**, 5147–5172.
20 F. D. Lewis, A. K. Thazhathveetil, T. A. Zeidan, J. Vura-Weis and M. R. Wasielewski, *J. Am. Chem. Soc.*, 2010, **132**, 444–445.
21 Y. Vyborna, M. Vybornyi, A. V. Rudnev and R. Häner, *Angew. Chem., Int. Ed.*, 2015, **54**, 7934–7938.
22 R. Häner, F. Garo, D. Wenger and V. L. Malinovskii, *J. Am. Chem. Soc.*, 2010, **132**, 7466–7471.
23 Y. Vyborna, M. Vybornyi and R. Häner, *J. Am. Chem. Soc.*, 2015, **137**, 14051–14054.
24 Y. Vyborna, M. Vybornyi and R. Häner, *Chem. Commun.*, 2017, **53**, 5179–5181.
25 C. D. Bösch, J. Jevric, N. Bürki, M. Probst, S. M. Langenegger and R. Häner, *Bioconjugate Chem.*, 2018, **29**, 1505–1509.
26 S. Rothenbühler, I. Iacovache, S. M. Langenegger, B. Zuber and R. Häner, *Nanoscale*, 2020, **12**, 21118–21123.
27 M. Kownacki, S. M. Langenegger, S.-X. Liu and R. Häner, *Angew. Chem., Int. Ed.*, 2019, **58**, 751–755.
28 M. R. Jones, N. C. Seeman and C. A. Mirkin, *Science*, 2015, **347**, 1260901.
29 F. H. Schacher, P. A. Rupar and I. Manners, *Angew. Chem., Int. Ed.*, 2012, **51**, 7898–7921.
30 A. Broggi, H. Kim, J. Jung, M. P. Bracciale, M. L. Santarelli, C. Kim and A. Marrocchi, *Macromol. Chem. Phys.*, 2017, **218**, 1–9.
31 P. R. Bohländer and H. A. Wagenknecht, *Org. Biomol. Chem.*, 2013, **11**, 7458–7462.
32 J. S. Huff, P. H. Davis, A. Christy, D. L. Kellis, N. Kandadai, Z. S. D. Toa, G. D. Scholes, B. Yurke, W. B. Knowlton and R. D. Pensack, *J. Phys. Chem. Lett.*, 2019, **10**, 2386–2392.
33 R. Feng, W. Shi, D. Wang, J. Wen, H. Li, S. Sun and Y. Xu, *Sci. Rep.*, 2017, **7**, 43491.
34 C. Luo, Q. Zhou, W. Lei, J. Wang, B. Zhang and X. Wang, *Supramol. Chem.*, 2011, **23**, 657–662.
35 O. A. Mass, C. K. Wilson, S. K. Roy, M. S. Barclay, L. K. Patten, E. A. Terpetschnig, J. Lee, R. D. Pensack, B. Yurke and W. B. Knowlton, *J. Phys. Chem. B*, 2020, **124**, 9636–9647.
36 L. I. Markova, V. L. Malinovskii, L. D. Patsenker and R. Häner, *Org. Biomol. Chem.*, 2012, **10**, 8944–8947.

37 H. Chen, M. S. Farahat, K.-Y. Law and D. G. Whitten, *J. Am. Chem. Soc.*, 1996, **118**, 2584–2594.
38 S. Das, K. G. Thomas, K. J. Thomas, V. Madhavan, D. Liu, P. v. Kamat and M. v. George, *J. Phys. Chem.*, 1996, **100**, 17310–17315.
39 D. Zhang, Y.-X. Zhao, Z.-Y. Qiao, U. Mayerhöffer, P. Spenst, X.-J. Li, F. Würthner and H. Wang, *Bioconjugate Chem.*, 2014, **25**, 2021–2029.
40 L. I. Markova, V. L. Malinovskii, L. D. Patsenker and R. Häner, *Chem. Commun.*, 2013, **49**, 5298–5300.
41 M. Madsen and K. v. Gothelf, *Chem. Rev.*, 2019, **119**, 6384–6458.
42 M. Kasha, *Radiat. Res.*, 1963, **20**, 55–70.
43 S. E. Boiadjiev and D. A. Lightner, *Monatsh. Chem.*, 2005, **136**, 489–508.
44 T. F. A. de Greef, M. M. J. Smulders, M. Wolffs, A. P. H. J. Schenning, R. P. Sijbesma and E. W. Meijer, *Chem. Rev.*, 2009, **109**, 5687–5754.